HHS Public Access

Author manuscript

Cancer Res. Author manuscript; available in PMC 2017 October 15.

Published in final edited form as:

Cancer Res. 2016 October 15; 76(20): 6107–6117. doi:10.1158/0008-5472.CAN-16-0621.

WWOX and p53 Dysregulation Synergize to Drive the Development of Osteosarcoma

Sara Del Mare[1], **Hussam Husanie**[1], **Ortal Iancu**[1], **Mohammad Abu-Odeh**[1], **Konstantinos Evangelou**[2], **Francesca Lovat**[3], **Stefano Volinia**[4], **Jonathan Gordon**[5], **Gail Amir**[6], **Janet Stein**[5], **Gary S. Stein**[5], **Carlo M. Croce**[3], **Vassilis Gorgoulis**[2,7,8,9], **Jane B. Lian**[4,*], and **Rami I. Aqeilan**[1,3,*]

[1]The Lautenberg Center for Immunology and Cancer Research, IMRIC, Faculty of Medicine, Hebrew University of Jerusalem, Israel 91220

[2]Department of Histology and Embryology, School of Medicine, University of Athens, Athens, Greece

[3]Department of Molecular Virology, Immunology and Medical Genetics (MVIMG), The Ohio State University Wexner Medical Center, Columbus, OH 43210, USA

Department of Morphology, Surgery and Experimental Medicine, University of Ferrara, Ferrara, Italy

[5]Department of Biochemistry, University of Vermont College of Medicine, Burlington, VT, 05405

[6]Department of Pathology, Hadassah University Hospital, Jerusalem 91220

[7]Biomedical Research Foundation of the Academy of Athens, Athens, Greece

[8]Faculty Institute of Cancer Sciences, University of Manchester, Manchester Academic Health Science Centre, Manchester, UK

[9]Manchester Centre for Cellular Metabolism, University of Manchester, Manchester Academic Health Science Centre, Manchester, UK

Abstract

Osteosarcoma (OS) is a highly metastatic form of bone cancer in adolescents and young adults which is resistant to existing treatments. Development of an effective therapy has been hindered by very limited understanding of the mechanisms of osteosarcomagenesis. Here, we used genetically engineered mice to investigate the effects of deleting the tumor suppressor *Wwox* selectively in either osteoblast progenitors or mature osteoblasts. Mice with conditional deletion of *Wwox* in pre-osteoblasts ($Wwox^{\Delta osx1}$) displayed a severe inhibition of osteogenesis accompanied by p53 upregulation, effects that were not observed in mice lacking *Wwox* in mature osteoblasts. Deletion of *p53* in $Wwox^{\Delta osx1}$ mice rescued the osteogenic defect. In addition, the $Wwox;p53^{\Delta osx1}$ double knockout mice developed poorly differentiated osteosarcomas that resemble human OS in histology, location, metastatic behavior, and gene expression. Strikingly, the development of

Author to whom correspondence should be addressed is Rami Aqeilan, ramiaq@mail.huji.ac.il.
*RIA and JBL acted as co-directors of the study.

Disclosure of Potential Conflicts of Interest. Non

osteosarcomas in these mice was greatly accelerated compared to mice lacking p53 only. In contrast, combined WWOX and p53 inactivation in mature osteoblasts did not accelerate osteosarcomagenesis compared to p53 inactivation alone. These findings provide evidence that a WWOX-p53 network regulates normal bone formation and that disruption of this network in osteoprogenitors results in accelerated OS. The *Wwox;p53*$^{\Delta osx1}$ double knockout establishes a new OS model with significant advancement over existing models.

Keywords

mouse model; osteosarcoma; WWOX; p53; genomic instability

Introduction

Osteosarcoma (OS) is the most common malignant bone tumor in adults and children (1,2). Sporadic human OS is characterized by complex chromosomal rearrangements, deletions, and amplifications, suggesting that genomic instability is a hallmark of the tumor. OS is highly aggressive and is associated with poor clinical outcomes, as it frequently metastasizes to the lungs. Patients with an autosomal recessive mutation of p53 (Li-Fraumeni syndrome) have a significantly higher incidence of OS and somatic mutation of p53 is frequently reported in sporadic OS (3,4). Importantly, restricted deletion of p53 in osteoblast progenitors results in the development of OS with 60% penetrance in the *Col3.6-Cre* mouse model (5) and 100% penetrance in *Osx1-Cre*$^{+}$ conditional knockout mice (6,7).

Since OS is characterized by high genomic complexity, it is useful to focus on the discovery of genes involved in the initiation and early progression of OS (8). Our recent work uncovered the role of the *WWOX* gene in OS and bone homeostasis (9,10). WWOX expression is altered by deletions or translocations in many cancer types, suggesting it acts as a tumor suppressor (11,12). Restoration of WWOX in many cancer cell lines, including OS cells, suppresses tumorigenicity (13). Conversely, *Wwox*$^{-/-}$ mice develop lesions resembling OS (14). Intriguingly, WWOX expression appears to be inversely associated with expression of RUNX2, the master regulator of osteoblastogenesis (10) and potential oncogene in OS and other metastatic cancers (15) (16).

To better elucidate the role of WWOX in osteoblast biology and in OS, we generated two conditional knockout mouse models in which WWOX is ablated specifically in either pre-osteoblasts (*Wwox*$^{\Delta Osx1}$) or fully mature osteoblasts (*Wwox*$^{\Delta Oc}$). Analysis of these mice revealed that WWOX is critical for normal osteoblast differentiation and that its co-inactivation together with that of p53 in pre-osteoblasts accelerates OS formation.

Materials and methods

Generation of *Wwox* conditional-knockout mice and *Wwox-p53* double knockout mice

The generation of *Wwox* conditional knock-out mice in osteoblast lineage cells was performed by crossing *Wwoxfl/fl* mice with osterix (*Osx1*)-Cre for deletion in mesenchymal progenitors committed to the bone formation (17), or with osteocalcin (*Oc*)-Cre mice for deletion in mature osteoblasts and osteocytes (18,19). Double-knockout (DKO) mice

(*Wwox/p53*$^{\Delta Osx1}$ [DKO$^{\Delta Osx1}$] or *Wwox/p53*$^{\Delta Oc}$ [DKO$^{\Delta Oc}$]) were generated by crossing single *Wwox* knockout mice with *p53fl/fl* mice (20). All experiments involving mice were approved by the Hebrew University Institutional Animal Care and Use Committee.

Histology and immunohistochemistry on human OS samples

Tissues were fixed in 10% neutral buffered-formalin and then paraffin embedded, sectioned, and stained with hematoxylin and eosin or with the desired antibody. All pathology was performed blinded to the sample genotype. Tumor specimen origin and pathological characteristics, immunohistochemistry procedure, and evaluation criteria were previously described (21,22). The immunoreactivity of WWOX was evaluated for percentage of positive cells and intensity of reactivity at high magnification. The intensity was evaluated as follows; 0 (no staining of any nuclear and cytoplasm at high magnification); 1, weak (only visible at high magnification); 2, moderate (easily visible at low magnification); and 3, strong (strongly positive at low magnification). The total score was obtained by multiplying the proportion and intensity scores, which ranged from 0–9. For further analysis, a cut-off point was established to separate the groups in terms of protein expression into a low expression group (staining patterns with total scores ≤4.5) and a high expression group (staining patterns with total scores>4.5).

Statistics

Results of *in vitro* and *in vivo* experiments were expressed as mean ± SD or SE. Student's *t*-test, was used to compare values of test and control samples. $P < 0.05$ indicates significant difference.

Detailed material and methods are presented in Supplementary information.

Results

Wwox ablation in osteoblast lineage cells results in delayed bone formation

Systemic *Wwox* null mice exhibit postnatal lethality, precluding studies of *Wwox* deletion effects in adult bony tissues (14). However, prior to their death at 2–3 weeks, pre-osteosarcoma lesions were identified in the limbs of these mice, and their bones showed severe osteopenia (9). To address the precise role of WWOX in bone and OS development, we generated two murine conditional *Wwox* knockout models. In the first, mice bearing floxed alleles of *Wwox* (19) were crossed to mice expressing Cre recombinase downstream of the *Osterix* (*Osx1*) promoter (*Osx1-Cre*$^{+}$), which is expressed in osteochondro mesenchymal progenitor cells (17), generating *Wwox*$^{\Delta Osx1}$ mice. In the second model (*Wwox*$^{\Delta Oc}$), *Wwox* ablation was driven by the *Osteocalcin* promoter (*Oc-Cre*$^{+}$), which is robustly expressed in fully mature osteoblasts (18). Hereafter, the models are referred to together as *Wwox*$^{\Delta OB}$ when describing findings that are identical in both lines of mice. *Wwox*$^{\Delta OB}$ mice were viable, fertile, and appeared grossly normal, with the exception of a slight growth delay in *Osx1-Cre*$^{+}$ animals compared with *Osx-Cre*$^{-}$ animals, although this difference diminished as the mice aged. To validate *Wwox*$^{\Delta OB}$ mouse models, we assessed *Wwox* levels by qPCR and immunoblot analyses in femurs (endochondral bone) and calvariae (membranous bone) (Fig. 1A,1D). *Wwox* levels were efficiently reduced in

Wwox$^{\Delta OB}$ mice compared to control mice or liver extracts. To determine whether *Wwox* ablation had an effect on homeostasis of long bones, microcomputed tomography (μCT) analyses was performed. Consistent with previous observations in *Wwox*-null mice (9), μCT imaging revealed a significant reduction in formation of trabecular bone with the number of trabeculae significantly decreased by 40% and trabecular spacing significantly increased by 33% in *Wwox*$^{\Delta Osx1}$ mice femurs at 1-month when compared to CTRL (*Osx1-Cre*-negative) (Fig. 1B) and HET (*Osx1-Cre*$^{+}$*;Wwox* $^{fl/+}$) femurs (Fig. S1A,B). After this period of rapid growth, the increase in trabecular spacing was maintained at 3- and 8-months of age, suggesting a striking delay in trabecular bone growth. Of note, HET mice had a similar phenotype as in CTRL mice, suggesting that the phenotype observed is not due to *Osx1* expression but to the actual inactivation of *Wwox*. In *Wwox*$^{\Delta Oc}$ mice, μCT analysis showed no phenotype at 1-month, though by 3-months trabecular numbers were decreased and trabecular spacing increased in *Wwox*$^{\Delta Oc}$ mice (Fig. 1E, S1D), indicating impaired bone formation in this mouse model as well. Indeed, qPCR analysis of whole femurs from 1-month old *Wwox*$^{\Delta Osx1}$ and 3-month old *Wwox*$^{\Delta Oc}$ mice revealed decreased expression of bone formation markers (Fig S1C,E) in *Wwox*$^{\Delta OB}$ compared to controls.

To further confirm the reduced bone mass in our results we performed quantification of serum P1NP levels as a surrogate marker of bone formation. As shown in Fig S1F, P1NP levels were significantly reduced in 1-month of *Wwox*$^{\Delta Osx1}$ mice relative to control. The same trend was observed in older *Wwox*$^{\Delta Osx1}$ mice though to a lesser extent. Consistent with μCT analysis, *Wwox*$^{\Delta OC}$ mice display reduced P1NP levels in 3-month old mice (Fig. S1F). In agreement with previous observations in *Wwox*-null mice (9), WWOX ablation in osteoblasts didn't affect osteoclast activity as assessed by serum CTX levels (Fig. S1G).

We next determined whether the impairment in bone formation is due to a cell-autonomous defect in osteoblast differentiation. Real-time-PCR of *ex vivo* calvariae cultures harvested at day 0, 7, 14 and 27 of differentiation revealed a significant downregulation of both early (*Runx2*, *Osx, ColIa1*) and late (*Oc*) osteogenesis markers (Fig. S2A,B) and decreased activity of ALP as well as absence of Alizarin Red staining, markers of differentiation and mineral deposition, respectively (Fig. 1C,1F). Our findings suggest that *Wwox* inactivation in osteoblasts is sufficient to negatively regulate the mineralization process. While ablation of WWOX in osteoblast lineage cells resulted in reduced bone mass due to impaired differentiation similar to that observed in *Wwox* null mice, we did not observe OS formation in *Wwox*$^{\Delta OB}$ mice.

Defects in differentiation of Wwox-deficient osteoprogenitors are partially rescued by p53 deletion

To uncover the possible mechanism(s) leading to both impaired bone formation and lack of OS formation by inactivation of WWOX, we considered key factors that are involved in regulation of both processes. One candidate is p53, which is considered a negative regulator of osteoblastogenesis (5) and is mutated in the majority of OSs (24). We first determined the levels of p53 and its target genes, during differentiation in control and *Wwox*$^{\Delta OB}$ calvarial osteoblasts. We found that differentiation dramatically downregulated both *Trp53* and *Cdkn1a* mRNA levels in control cells, consistent with the known role of p53 in inhibiting

osteoblast differentiation (5). In sharp contrast, osteoblasts isolated from *Wwox*$^{\Delta Osx1}$ mice displayed significantly higher activity of p53 upon differentiation relative to those from control mice (Fig 2A). At 21 days post-differentiation, *Wwox*$^{\Delta Osx1}$ calvarial osteoblasts and femurs displayed increased expression of *Trp53*, *Cdkn1a*, *Bax*, *and Puma* levels compared to control cells (Fig. 2B). Intriguingly, osteoblasts isolated from *Wwox*$^{\Delta Oc}$ did not exhibit activation of p53 (Fig 2B). These data suggest that *Wwox* deficiency in osteoprogenitors, but not in mature osteoblasts, activates p53, likely leading to inhibition of osteoblast differentiation.

These results prompted us to examine whether deleting p53 in *Wwox*$^{\Delta Osx1}$ cells would rescue their differentiation defect. To this end, we bred *Wwox*$^{\Delta Osx1}$ with *p53fl/fl* mice to generate mice lacking both WWOX and p53 (*DKO*$^{\Delta Osx1}$) specifically in committed osteoblasts (*Wwox;p53*$^{\Delta Osx1}$). Calvariae osteoblasts isolated from newborn pups of control, *Wwox*$^{\Delta Osx1}$ and DKO mice were induced to differentiate and osteogenic parameters were measured. We found that DKO preosteoblasts expressed differentiation markers at levels similar to control cells (Fig 2C), were stained by Alizarin Red (Fig. 2D), and displayed increased ALP activity upon differentiation (Fig. 2E) when compared to *Wwox*$^{\Delta Osx1}$ preosteoblasts.

We next determined the effect of *Wwox* ablation on differentiation of p53-negative osteoblasts. Bone marrow-mesenchymal stem cells (BMSCs) were isolated from *p53*$^{\Delta Osx1}$ and DKO mice and were induced to differentiate. BMSCs from DKO mice showed a general decrease of both early and late osteogenic markers after 7 days (early) or 21 days (late) of differentiation (Fig. 2F) and less pronounced staining with Alizarin Red (Fig. 2H). This is in contrast to the complete ablation of osteogenesis markers observed in differentiated BMSCs from the *Wwox*$^{\Delta Osx1}$ mice, likely due to the absence of negative regulation by p53.

Wwox deletion in *p53*$^{\Delta Oc}$ BMSCs led to a striking increase in *Runx2* expression relative to *p53*$^{\Delta Oc}$ BMSCs, promoting commitment of mesenchymal stem cells to osteogenesis, and accompanied by markers of accelerated differentiation (Fig. 2G,2I). These results indicate that unlike the effect of the DKO earlier in development, combined WWOX and p53 ablation late in osteoblast development does not affect osteogenesis. Taken together, we conclude that *Wwox* loss in early osteoprogenitors is associated with upregulation of p53, leading to impaired differentiation. These results suggest that WWOX and p53 co-regulate bone formation.

Combined inactivation of WWOX and p53 in committed osteoblasts accelerates osteosarcomagenesis

Inactivation of the p53 pathway is known to be a central event in OS formation (3,4) and loss of p53 in developing osteoblasts in the *Osx1-Cre*$^{+}$*;p53*$^{fl/fl}$ (*p53*$^{\Delta Osx1}$) mouse model results in OS with complete penetrance at ~12 months of age (6,7). The effects of p53 conditional deletion in mature osteoblasts on OS formation are unknown. Since WWOX and p53 appear to co-regulate osteogenesis, we investigated whether they also function coordinately in suppressing tumor formation by assessing OS formation in mice lacking both WWOX and p53 under *Osx1*- or *Oc*- promoters. Mice were monitored closely and OSs were detected primarily by palpation. In addition, a group of mice underwent μPET scans

(Fig. S3) to detect early tumor formation. We found that combined inactivation of *Wwox* and *p53* using *Osx1-Cre* accelerates OS formation. DKO$^{\Delta Osx1}$ mice exhibited complete tumor penetrance starting at 4 months, while *p53*$^{\Delta Osx1}$ mice developed OS 4–6 months later (Fig. 3A). There was a 93.7% penetrance of OS development in *Osx1Cre*$^{+}$*;Wwox*$^{fl/+}$*p53*$^{fl/fl}$ mice, 75% in *Osx1Cre*$^{+}$*;Wwox*$^{fl/fl}$*p53*$^{fl/+}$ mice, and 63.6% in *p53*$^{\Delta Osx1}$ mice (Table S1). We analyzed a total of 11 *p53*$^{\Delta Osx1}$ mice, 23 *DKOs*, 16 *Osx1-Cre*$^{+}$*Wwox*$^{fl/+}$*p53*$^{fl/fl}$, 9 *Osx1-Cre*$^{+}$*Wwox*$^{fl/fl}$*p53*$^{fl/+}$ and 6 *Osx1-Cre*$^{+}$*Wwox*$^{fl/+}$*p53*$^{fl/+}$ mice (Table S1). Histological evaluation of these tumors revealed OS of osteoblastic origin of grade III/IV with variability in the appearance of bone tissues (Fig. 3B). OS often spread with extra osseous extension from the site of origin into the muscle and soft tissue. The tumor bone was osteoid of woven bone formed by the tumor cells. The most frequent sites of tumors in the OS-bearing mice were the ribs and vertebrae (51%), followed by hind leg and hip (22%), and the jaw (20%) (Fig. S4).

Interestingly, there was no significant difference between the development of OS in the DKO and *Osx1Cre*$^{+}$*;Wwoxfl/+;p53fl/fl* (referred to as HET). These results led us to question whether the other allele of *Wwox* was lost in the tumors. To this end, we examined the expression of WWOX in these tumors by immunohistochemistry. We found that WWOX expression in HET tumors is lost in more than 70% of the specimens examined, suggesting loss of heterozygosity (LOH), a hallmark of tumor suppressor genes. Additionally, WWOX expression was lost in ~40% of *p53*$^{\Delta Osx1}$ tumors analyzed, suggesting that *Wwox* inactivation can occur as a result of p53 loss (Fig S5A). Representative images of *Wwox* immunostaining and levels in different tumors and cells are shown in Fig. S5.

Importantly, cells derived from DKO$^{\Delta Osx1}$ show a more aggressive proliferation rate when compared to *p53*$^{\Delta Osx1}$ or *Wwox* HET cells which display intact WWOX expression (Fig S5C, S6). Metastases were detected in 20% of DKO$^{\Delta Osx1}$ and HET while in 12% of *p53*$^{\Delta Osx1}$ mice. Together, these data indicate that combined inactivation of tumor suppressors WWOX and p53 in osteoprogenitors accelerates osteosarcomagenesis. In contrast to this combinatorial effect of the double knockout in pre-osteoblasts, the development and progression of OS in mice lacking both WWOX and p53 in mature osteoblasts (DKO$^{\Delta Oc}$; *Oc-Cre*$^{+}$*;Wwox*$^{fl/fl}$*p53*$^{fl/fl}$) was not significantly different from single p53 knockout mice (*p53*$^{\Delta Oc}$) (Fig. 3C,D and Table S2). In mice of both these genotypes, OS was highly aggressive (stage III/IV), metastatic, and invasive with penetrance of ~80% (Table S2). We conclude that the combined activities of WWOX and p53 in early osteoprogenitors exert critical regulation to prevent their transformation into OS.

Differentiation status of tumors and cells derived from DKO$^{\Delta Osx1}$ mice

High-grade OS cells have reduced expression of bone markers, suggesting that they are undifferentiated and aggressive tumor cells (25). To examine the relationship between accelerated OS formation and reduced differentiation of pre-osteoblasts, we compared osteogenic differentiation of tumor cells in *p53*$^{\Delta Osx1}$ and *DKO*$^{\Delta Osx1}$ mice. Levels of late osteogenic marker mRNAs in DKO$^{\Delta Osx1}$ tumors were dramatically downregulated relative to *p53*$^{\Delta Osx1}$ tumors (Fig. 3E). Furthermore, weak Sirius-Red staining of tumor tissues confirmed a significant reduction in levels of collagen, a marker of differentiation, in the

majority (70%) of DKO$^{\Delta Osx1}$ tumors (Fig. 3F). In contrast, most (66%) *p53*$^{\Delta Osx1}$ OS strongly stained with Sirius-Red. Moreover, DKO$^{\Delta Osx1}$ tumor–derived cells failed to differentiate (Fig. 3G) or to form mineralized bone (Fig 3H,I) when compared to *p53*$^{\Delta Osx1}$-derived tumor cells. Consistent with the hypothesized function of p53 as a negative regulator of osteoblast differentiation (5), high levels of osteoblast markers were found in *p53*$^{\Delta Osx1}$ tumor cells, while DKO$^{\Delta Osx1}$ tumor cells exhibited poor differentiation. Restoring WWOX expression in DKO$^{\Delta Osx1}$ tumor cells improved, at least in part, their ability to differentiate and mineralize (Fig. S7). These results support the concept that co-inactivation of WWOX and p53 accelerates OS formation by increasing proliferation and compromising osteoblast differentiation.

Transcriptomic analysis reveals mouse and human OS share genetic abnormalities

We performed RNA sequencing to assess and compare genetic dysregulation in DKO and *p53*$^{\Delta Osx1}$ tumors. The large group of genes altered in DKO OS is enriched for genes involved in DNA damage response (DDR), cell adhesion, and cell motility pathways (Table S4). We compared the results of the DKO RNA-sequencing with our previous human OS Affymetrix analysis (26) (Fig 4A). The comparison revealed 171 genes that are similarly altered in human and mouse OS. Subsets of these genes related to cancer and osteogenesis were validated by qPCR (Fig. 4B). Functional clustering of these genes using DAVID Annotation revealed that many are involved in the regulation of cell metabolism (*POLE4*, *PGM5*, *PDK2*), cell adhesion (*ALCAM*, *FN1*, *ITGAE*), apoptosis (*SNAI2*, *EAF2*, *DAP3*), cell cycle (*AGTRAP*, *DCTN1*, *TXNL4B*), DNA damage (*RAD23*, *FANCb* and *FBXO31*), and bone development (*FOXC1*, *GLI1*, *FHL2*), among others (Table S5). These data further confirm that our murine OS model recapitulates human OS.

Increased RUNX2 activity in tumors and cells derived from DKO$^{\Delta Osx1}$ mice

Several genes that emerged from the RNA-sequencing analysis are targets of RUNX2, including *ALCAM*, *RAD23*, *AGTRAP* and *NFATC21p* (15,27). We previously demonstrated that WWOX protein physically interacts with RUNX2 and can inhibit its transactivation activity in normal osteoblasts (9). Moreover, van der Deen M et al. have shown that several genes involved in cell adhesion and motility in OS cells are direct targets of RUNX2 (15). As shown in Fig 4C, we found that tumor-related RUNX2 target genes are significantly overexpressed in DKO$^{\Delta Osx1}$ tumors and cells compared to *p53*$^{\Delta Osx1}$. These findings indicate that *Wwox* inactivation is accompanied by upregulation of RUNX2 activity that is involved in tumor proliferation and invasion, which may render the tumors more aggressive.

DNA Damage Response (DDR) is impaired in DKO$^{\Delta Osx1}$ tumor cells

One of the main obstacles in the treatment of OS is chemoresistance, likely due to a failure of DDR activation and impairment of the p53 pathway. Our transcriptomic analysis revealed altered expression of genes involved in DDR, so we set to examine the response to OS-relevant drugs such as doxorubicin and cisplatin in DKO$^{\Delta Osx1}$ versus *p53*$^{\Delta Osx1}$ tumor cells. We found that DKO$^{\Delta Osx1}$ tumor cells are more resistant to chemotherapy drugs relative to *p53*$^{\Delta Osx1}$ cells (Fig. 5A), consistent with previous observations that WWOX loss is associated with increased resistance to cisplatin (28). Recently, it was demonstrated that

WWOX loss is associated with impaired DDR upon induction of double strand breaks (DSBs) (29). Therefore, we addressed whether DDR efficiency is affected in OS cells isolated from DKO$^{\Delta Osx1}$ or *p53*$^{\Delta Osx1}$ mice. We examined cells for the presence of γH2AX foci, an early marker of DSBs (30), at different time points after treatment with neocarzinostatin (NCS), a well-characterized inducer of DSBs (31). Using immunofluorescence, we observed that DKO$^{\Delta Osx1}$ cells display elevated levels of spontaneous γH2AX foci formation (Fig. 5B,C). Moreover, upon induction of DSBs, DKO$^{\Delta Osx1}$ cells exhibited a transient delay in the formation of γH2AX foci at early time-points following NCS. The persistence of γH2AX is also an indicator of failed DNA repair. At 24–48 hours after NCS treatment, DKO cells exhibited sustained γH2AX foci, in contrast to *p53*$^{\Delta Osx1}$ cells (Fig. 5B,C). These results indicate that combined p53 and *Wwox* inactivation is associated with impaired DDR.

To validate our results in a different system and better understand the role of WWOX in DDR, we examined DNA DSBs in WWOX-depleted MC3T3 cells, an immortalized preosteoblasts, by performing a comet assay upon gamma radiation (Fig. 5D,E). We measured tail-moment of individual cells, which provides an indirect measurement of DNA DSBs. As expected, depletion of WWOX was associated with increased DSBs after induction of DNA-damage (Fig. 5D,E). These results suggest that *WWOX* depletion enhances genomic instability upon DNA damage.

Since OS cells are known to display a complex karyotype, we next performed karyotype analysis of mouse cells from tumors. Twenty metaphases of each cell type were examined, revealing a higher number of spontaneous chromosomal breaks in DKO$^{\Delta Osx1}$ or HET cells (6 breaks per cell out of 20 cells; 6/20) compared to *p53*$^{\Delta Osx1}$ cells (3/20) (Fig. S8), further suggesting that WWOX loss is associated with genomic instability.

Loss of WWOX in human OS is associated with inactivation of p53 and impaired DDR

To investigate the relevance of a p53/WWOX association in human OS, immunohistochemistry for WWOX was performed on 57 human OS cases with known p53 status (21). Twenty cases harbored p53 mutations, while the rest were p53 wt (21). A panel of representative images of the staining is shown in Fig. 6A. A striking proportion (24/37) of p53 wt cases displayed positive WWOX immunostaining (total scores >4.5), while almost all (17/20) p53 mutant cases exhibit little or no WWOX expression (total scores ≤4.5) (Fig 6B). A cluster (n=13) of p53 wt/WWOX negative cases was also evident. Statistically significant difference were found when comparing WWOX immunohistochemical scoring values between p53 wt (average score=4.7) and p53 mutant samples (average score=1.75) (Fig. 6C). These data show that tumors with intact p53 (negative staining) tend to be positive for WWOX expression, while most cases we examined with inactivated p53 (positive staining) also have inactivated or greatly reduced WWOX expression. Analysis of DDR markers in relation to WWOX expression in human OS reveals a clear trend of impaired DDR in WWOX negative-cases and *vice-versa* (Fig 6D). Together with our observations in mouse models, these data suggest that co-inactivation of WWOX and p53 is a common event in OS.

Discussion

In this study we have established the role of WWOX in osteogenesis and as a suppressor of OS development. Inactivation of *Wwox* in osteprogenitor cells in $Wwox^{\Delta Osx1}$ mice activated p53, resulting in defective osteoblast differentiation and decreased tumor formation. Significantly, the combined loss of WWOX and p53 in mouse pre-osteoblasts, but not mature osteoblasts, accelerated OS formation and progression. Our findings indicate that WWOX loss in early osteoblast differentiation is associated with impaired DDR, which could cooperate with enhanced RUNX2 activity to cause aggressive high-grade OS formation. These findings represent the first *in vivo* evidence that WWOX loss alters osteoprogenitor phenotype and directly contributes to OS formation. Based on our previous observations of *Wwox* null mice it became apparent that WWOX has crucial role in bone homeostasis since its loss leads to osteopenia (9). In this new model, WWOX is absent from early and late stages of osteoblast lineage cells, and hence the phenotype is stronger (9). In the new conditional KO models, where WWOX is specifically depleted in a particular population, we detected a transient reduction in bone mass and impaired osteoblast differentiation that was compensated with age (Fig 2, Fig S1,S2). Additionally, stromal cells in the conditional KO models do express WWOX which could contribute to the subtle observed phenotype. Should WWOX be conditionally eliminated in the mesenchymal stem cell compartment, using for example Prx1-Cre, it may result in a more profound effect that possibly resemble the full phenotype as observed in the null model. Importantly, our findings have established a role for WWOX in supporting osteoblast differentiation and that its loss in OS cells promotes a highly tumorigenic phenotype.

Reduction or absence of WWOX is a common event in human OS (10,32). To better characterize the function of WWOX in osteogenesis, we studied the contribution of WWOX ablation in specific stages of osteoblasts maturation. These studies revealed that inactivation of WWOX in osteoprogenitors promote p53 checkpoint signaling, inhibiting proper osteoblast differentiation, as well as tumor formation. Experiments in which expression of both WWOX and p53 is ablated in osteoprogenitors revealed that these genetic lesions can synergize to enhance OS development. In these double knockout mice, osteoblast differentiation is resumed to a certain level and tumors emerge with aggressive traits resembling human OS.

The mechanism by which WWOX expression modulates p53 levels is unknown. Physical and functional interactions between WWOX and p53 have previously been reported to promote mitochondrial apoptosis (33,34). Additionally, WWOX loss might render the genome less stable, which could lead to p53 activation (29,35). Subsequent genomic instability caused by WWOX loss, and likely other tumor suppressor genes, could lead to mutation(s) in p53 and emergence of OS. OS penetrance data reveals synergy between *Trp53* and *Wwox:* while OS penetrance in $p53^{\Delta Osx1}$ mice is 63%, in $Wwox;p53^{\Delta Osx1}$ mice it is almost 100%, highlighting the significance of a WWOX-p53 co-regulatory pathway in normal cells that is dysregulated in tumor cells. Our results differ from previous reports, perhaps due to differences in genetic backgrounds (25). Intriguingly, when comparing $p53^{\Delta Osx1}$ mice and $Osx1Cre^{+};Wwox^{fl/fl};p53^{fl/+}$, we observed similar pattern of survival (Fig 3A) though higher penetrance (Table S1) suggesting that WWOX loss might promote p53

LOH and appearance of more aggressive tumors. Loss of WWOX was also observed in *Osx1-Cre*$^{+}$;*Wwox* $^{fl/+}$;*p53*$^{fl/fl}$ OS suggesting its LOH. These findings underscore that functional loss of WWOX promotes tumor development directly from early stage osteoblast lineage cells.

Interestingly, our data indicate that WWOX deletion in mature osteoblasts using *Oc-Cre* does-not activate the p53 checkpoint, though it results in reduced osteoblast differentiation, suggesting that other factors play important roles in this context. Although Osteocalcin-expressing osteoblasts are thought to be non-cycling, they do form tumors upon *p53* and *Rb1* deletion (36). Our report is the first showing that deletion of p53 in mature osteoblasts (*p53*$^{\Delta Oc}$) is associated with high-grade OS. This is not surprising in light of recent evidence that structural and functional impairment of p53 is probably the most common pathological event in OS (3,4).

The exact cell of origin for OS remains to be definitively identified. Our *DKO*$^{\Delta Osx1}$ and *DKO*$^{\Delta Oc}$ mouse models support the hypothesis that OS arises from a committed osteoblastic lineage cell rather than from completely undifferentiated mesenchymal stem cells. This in line with data from other experimental models that favors an osteoblast population as the cell of origin (25,37,38). Nevertheless, OS is a heterogeneous disease with a very complex karyotype, suggesting that different genotypic and cellular anomalies could contribute to this variability.

The OS formed in *Wwox/p53*$^{\Delta Osx1}$ (*DKO*$^{\Delta Osx1}$) mice share several key features with human OS as compared to p53$^{\Delta Osx1}$ mouse model. First, the murine tumors in *Wwox/p53*$^{\Delta Osx1}$ mice are more aggressive and are characterized by a highly proliferative and poorly differentiated state; reduced osteocalcin levels and collagen deposition. Second, several differentially expressed genes identified in tumors of DKO$^{\Delta Osx1}$ mice have also been well-documented in human OS, including genes involved in DNA damage, cell metabolism, and cell adhesion. Of particular interest, many RUNX2 target genes involved in cell migration, adhesion, and proliferation are upregulated upon WWOX loss in human OS (27). Proteomic studies recently showed that RUNX2 forms functional complexes with several proteins to mount an integrated response to DNA damage (39). Our results lead us to speculate that WWOX has differential effects on RUNX2 binding at promoters of selected genes. Similarly, previous work has suggested that the absence of normal regulation of RUNX2 in osteoblasts converts RUNX2 from a differentiation and tumor suppressor factor to one that promotes tumor growth and metastasis. Lengner et al. showed that Mdm2-null osteoblast progenitor cells deleted for Mdm2 have elevated p53 activity and reduced proliferation (5), while p53-null osteoprogenitor cells have increased proliferation, increased expression of RUNX2 and increased osteoblast maturation. In this context, our findings reveal that both WWOX and p53 loss are associated with increased RUNX2 activity, increased proliferation and increased tumorigenic potential.

Third, WWOX loss is associated with genomic instability and complex karyotype in human OS. We have shown recently that loss of WWOX is associated with impaired DDR (29,35), which could contribute to aggressive OS development. Considering that genomic analysis has revealed profound genomic instability and heterogeneity among human OS patients,

with nearly universal *TP53* somatic structural variations (3,4), our findings suggest that DKO$^{\Delta Osx1}$ mouse is a useful tool to study human OS. Aberrations in *TP53* were suggested to reflect preexisting, p53 deficiency-independent genomic instability in OS (3). Whether WWOX loss could facilitate this genomic instability *in vivo* has yet to be determined. Moreover, the tumors in DKO$^{\Delta Osx1}$ mice have impaired DNA repair and loss of p53 effector function suggests they will be difficult to eliminate with chemotherapy, and indeed, our analysis demonstrates that DKO$^{\Delta Osx1}$ cells display increased chemoresistance.

Lastly, we found a significant correlation between WWOX expression and p53 status in human OS specimens. In fact, the majority of human tumors that display a non-functional mutated form of p53 showed little or no immunostaining for WWOX, suggesting that WWOX inactivation together with p53 mutation is a common event in human OS, probably rendering it more aggressive.

To conclude, we report here a potent tumor suppressor role of WWOX in OS development *in vivo*, resulting from a mechanism that couples WWOX loss-of-function to p53 activity. Due to the strong similarity between murine OS in the *p53/Wwox* knockout model and human OS, this model provides a valuable platform for addressing the molecular genetics of OS and developing novel therapeutic strategies.

Acknowledgments

We are grateful for the Aqeilan lab members for fruitful discussions. This work was supported in part by the BSF grant (#2011300) to R.I.A, J.B.L., G.S and J. S., by P01 Cancer grant P01 CA82834 NIH/NCI to G.S. and R37 DE012528 NIH/NIDCR to J.B.L. V.G. and K.E. are financially supported by the Greek GSRT program of Excellence II (Aristeia II).

References

1. Ottaviani G, Jaffe N. The etiology of osteosarcoma. Cancer Treat Res. 2009; 152:15–32. [PubMed: 20213384]
2. Ottaviani G, Jaffe N. The epidemiology of osteosarcoma. Cancer Treat Res. 2009; 152:3–13. [PubMed: 20213383]
3. Chen X, Bahrami A, Pappo A, Easton J, Dalton J, Hedlund E, et al. Recurrent somatic structural variations contribute to tumorigenesis in pediatric osteosarcoma. Cell Rep. 2014; 7(1):104–112. [PubMed: 24703847]
4. Perry JA, Kiezun A, Tonzi P, Van Allen EM, Carter SL, Baca SC, et al. Complementary genomic approaches highlight the PI3K/mTOR pathway as a common vulnerability in osteosarcoma. Proc Natl Acad Sci U S A. 2014; 111(51):E5564–E5573. [PubMed: 25512523]
5. Lengner CJ, Steinman HA, Gagnon J, Smith TW, Henderson JE, Kream BE, et al. Osteoblast differentiation and skeletal development are regulated by Mdm2-p53 signaling. J Cell Biol. 2006; 172(6):909–921. [PubMed: 16533949]
6. Walkley CR, Qudsi R, Sankaran VG, Perry JA, Gostissa M, Roth SI, et al. Conditional mouse osteosarcoma, dependent on p53 loss and potentiated by loss of Rb, mimics the human disease. Genes Dev. 2008; 22(12):1662–1676. [PubMed: 18559481]
7. Berman SD, Calo E, Landman AS, Danielian PS, Miller ES, West JC, et al. Metastatic osteosarcoma induced by inactivation of Rb and p53 in the osteoblast lineage. Proceedings of the National Academy of Sciences of the United States of America. 2008; 105(33):11851–11856. [PubMed: 18697945]

8. Moriarity BS, Otto GM, Rahrmann EP, Rathe SK, Wolf NK, Weg MT, et al. A Sleeping Beauty forward genetic screen identifies new genes and pathways driving osteosarcoma development and metastasis. Nat Genet. 2015; 47(6):615–624. [PubMed: 25961939]
9. Aqeilan RI, Hassan MQ, de Bruin A, Hagan JP, Volinia S, Palumbo T, et al. The WWOX tumor suppressor is essential for post-natal survival and normal bone metabolism. J Biol Chem. 2008; 283(31):21629–21639. [PubMed: 18487609]
10. Kurek KC, Del Mare S, Salah Z, Abdeen S, Sadiq H, Lee SH, et al. Frequent attenuation of the WWOX tumor suppressor in osteosarcoma is associated with increased tumorigenicity and aberrant RUNX2 expression. Cancer Res. 2010; 70(13):5577–5586. [PubMed: 20530675]
11. Gardenswartz A, Aqeilan RI. WW domain-containing oxidoreductase's role in myriad cancers: Clinical significance and future implications. Experimental Biology and Medicine. 2014; 239(3): 253–263. [PubMed: 24510053]
12. Paige AJ, Taylor KJ, Taylor C, Hillier SG, Farrington S, Scott D, et al. WWOX: a candidate tumor suppressor gene involved in multiple tumor types. Proc Natl Acad Sci U S A. 2001; 98(20):11417–11422. [PubMed: 11572989]
13. Del Mare S, Kurek KC, Stein GS, Lian JB, Aqeilan RI. Role of the WWOX tumor suppressor gene in bone homeostasis and the pathogenesis of osteosarcoma. American journal of cancer research. 2011; 1(5):585–594. [PubMed: 21731849]
14. Aqeilan RI, Trapasso F, Hussain S, Costinean S, Marshall D, Pekarsky Y, et al. Targeted deletion of Wwox reveals a tumor suppressor function. Proc Natl Acad Sci U S A. 2007; 104(10):3949–3954. [PubMed: 17360458]
15. van der Deen M, Akech J, Lapointe D, Gupta S, Young DW, Montecino MA, et al. Genomic promoter occupancy of runt-related transcription factor RUNX2 in Osteosarcoma cells identifies genes involved in cell adhesion and motility. J Biol Chem. 2012; 287(7):4503–4517. [PubMed: 22158627]
16. Pratap J, Lian JB, Stein GS. Metastatic bone disease: role of transcription factors and future targets. Bone. 2011; 48(1):30–36. [PubMed: 20561908]
17. Rodda SJ, McMahon AP. Distinct roles for Hedgehog and canonical Wnt signaling in specification, differentiation and maintenance of osteoblast progenitors. Development. 2006; 133(16):3231–3244. [PubMed: 16854976]
18. Zhang M, Xuan S, Bouxsein ML, von Stechow D, Akeno N, Faugere MC, et al. Osteoblast-specific knockout of the insulin-like growth factor (IGF) receptor gene reveals an essential role of IGF signaling in bone matrix mineralization. J Biol Chem. 2002; 277(46):44005–44012. [PubMed: 12215457]
19. Abdeen SK, Del Mare S, Hussain S, Abu-Remaileh M, Salah Z, Hagan J, et al. Conditional inactivation of the mouse Wwox tumor suppressor gene recapitulates the null phenotype. Journal of cellular physiology. 2013; 228(7):1377–1382. [PubMed: 23254685]
20. Jonkers J, Meuwissen R, van der Gulden H, Peterse H, van der Valk M, Berns A. Synergistic tumor suppressor activity of BRCA2 and p53 in a conditional mouse model for breast cancer. Nature genetics. 2001; 29(4):418–425. [PubMed: 11694875]
21. Liontos M, Niforou K, Velimezi G, Vougas K, Evangelou K, Apostolopoulou K, et al. Modulation of the E2F1-driven cancer cell fate by the DNA damage response machinery and potential novel E2F1 targets in osteosarcomas. Am J Pathol. 2009; 175(1):376–391. [PubMed: 19541929]
22. Aqeilan RI, Hagan JP, Aqeilan HA, Pichiorri F, Fong LY, Croce CM. Inactivation of the Wwox Gene Accelerates Forestomach Tumor Progression In vivo. Cancer Res. 2007; 67(12):5606–5610. [PubMed: 17575124]
23. Trapnell C, Hendrickson DG, Sauvageau M, Goff L, Rinn JL, Pachter L. Differential analysis of gene regulation at transcript resolution with RNA-seq. Nat Biotechnol. 2013; 31(1):46–53. [PubMed: 23222703]
24. Mirabello L, Yeager M, Mai PL, Gastier-Foster JM, Gorlick R, Khanna C, et al. Germline TP53 variants and susceptibility to osteosarcoma. J Natl Cancer Inst. 2015; 107(7)
25. Jones KB. Osteosarcomagenesis: modeling cancer initiation in the mouse. Sarcoma. 2011; 2011:694136. [PubMed: 21403899]

26. Jones KB, Salah Z, Del Mare S, Galasso M, Gaudio E, Nuovo GJ, et al. miRNA signatures associate with pathogenesis and progression of osteosarcoma. Cancer Res. 2012; 72(7):1865–1877. [PubMed: 22350417]
27. Wu H, Whitfield TW, Gordon JA, Dobson JR, Tai PW, van Wijnen AJ, et al. Genomic occupancy of Runx2 with global expression profiling identifies a novel dimension to control of osteoblastogenesis. Genome Biol. 2014; 15(3):R52. [PubMed: 24655370]
28. Salah Z, Bar-mag T, Kohn Y, Pichiorri F, Palumbo T, Melino G, et al. Tumor suppressor WWOX binds to DeltaNp63alpha and sensitizes cancer cells to chemotherapy. Cell Death Dis. 2013; 4:e480. [PubMed: 23370280]
29. Abu-Odeh M, Salah Z, Herbel C, Hofmann TG, Aqeilan RI. WWOX, the common fragile site FRA16D gene product, regulates ATM activation and the DNA damage response. Proc Natl Acad Sci U S A. 2014; 111(44):E4716–E4725. [PubMed: 25331887]
30. Rogakou EP, Pilch DR, Orr AH, Ivanova VS, Bonner WM. DNA double-stranded breaks induce histone H2AX phosphorylation on serine 139. The Journal of biological chemistry. 1998; 273(10): 5858–5868. [PubMed: 9488723]
31. DeGraff WG, Krishna MC, Kaufman D, Mitchell JB. Nitroxide-mediated protection against X-ray- and neocarzinostatin-induced DNA damage. Free Radic Biol Med. 1992; 13(5):479–487. [PubMed: 1459474]
32. Yang J, Cogdell D, Yang D, Hu L, Li H, Zheng H, et al. Deletion of the WWOX gene and frequent loss of its protein expression in human osteosarcoma. Cancer Lett. 2010; 291(1):31–38. [PubMed: 19896763]
33. Chang NS. A potential role of p53 and WOX1 in mitochondrial apoptosis (review). Int J Mol Med. 2002; 9(1):19–24. [PubMed: 11744990]
34. Chang NS, Doherty J, Ensign A, Lewis J, Heath J, Schultz L, et al. Molecular mechanisms underlying WOX1 activation during apoptotic and stress responses. Biochem Pharmacol. 2003; 66(8):1347–1354. [PubMed: 14555208]
35. Abu-Odeh M, Heerema N, Aqeilan RI. WWOX modulates the ATR-mediated DNA damage checkpoint response. Oncotarget. 2015 In press.
36. Quist T, Jin H, Zhu JF, Smith-Fry K, Capecchi MR, Jones KB. The impact of osteoblastic differentiation on osteosarcomagenesis in the mouse. Oncogene. 2015; 34(32):4278–4284. [PubMed: 25347737]
37. Mutsaers AJ, Walkley CR. Cells of origin in osteosarcoma: mesenchymal stem cells or osteoblast committed cells? Bone. 2014; 62:56–63. [PubMed: 24530473]
38. Uluckan O, Bakiri L, Wagner EF. Characterization of mouse model-derived osteosarcoma (OS) cells in vitro and in vivo. Methods Mol Biol. 2015; 1267:297–305. [PubMed: 25636475]
39. Yang S, Quaresma AJ, Nickerson JA, Green KM, Shaffer SA, Imbalzano AN, et al. Subnuclear domain proteins in cancer cells support the functions of RUNX2 in the DNA damage response. J Cell Sci. 2015; 128(4):728–740. [PubMed: 25609707]

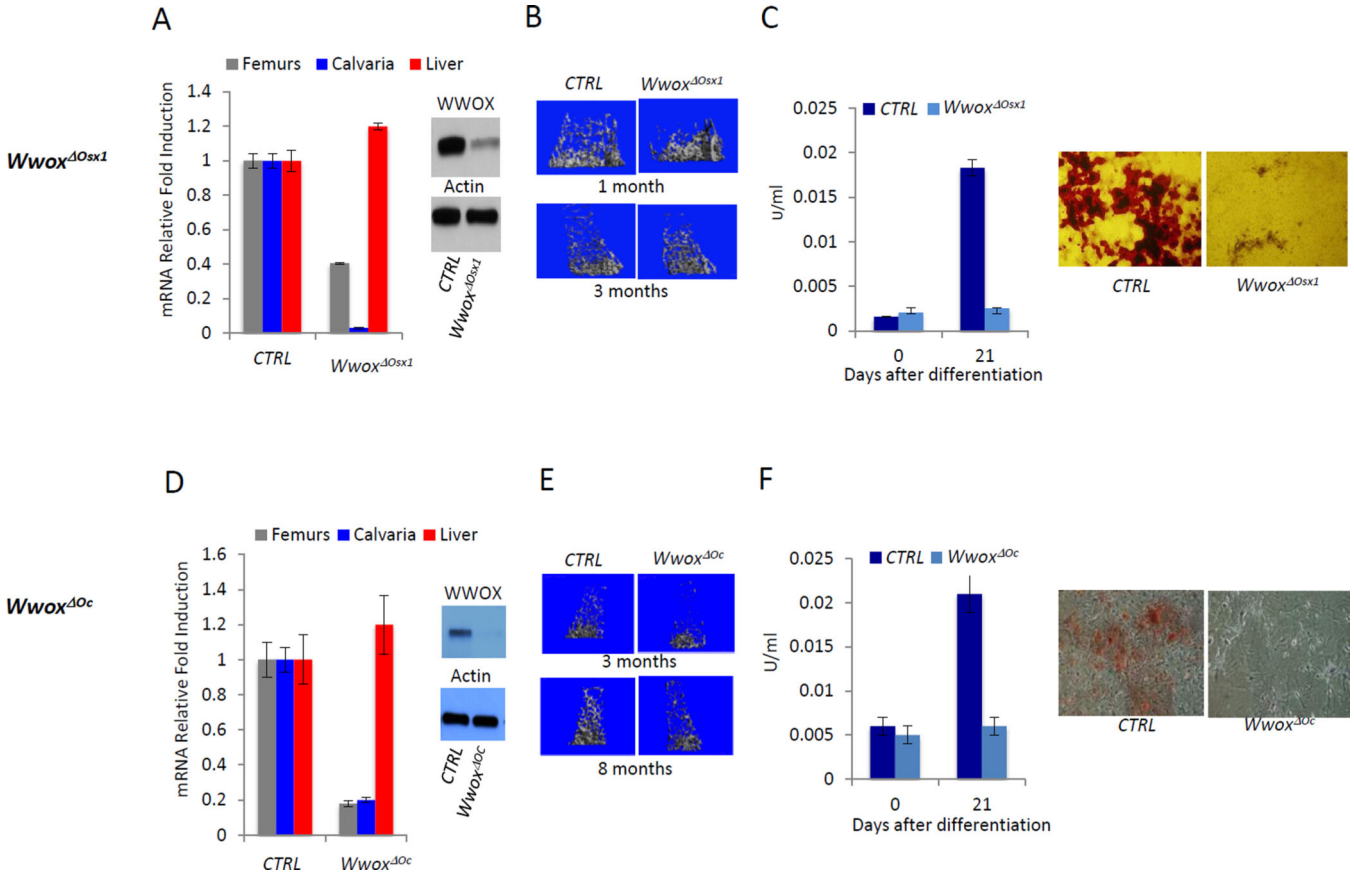

Figure 1. Characterization of *Wwox*$^{\Delta OB}$ conditional knockout mice

A. *Wwox* expression in femurs of CTRL and *Wwox*$^{\Delta Osx1}$ mice as assessed by qPCR on femur, calvaria and liver (left panel). Right panel shows immunoblot analysis of calvaria isolated from these mice. **B**. µCT three-dimensional images of control and *Wwox*$^{\Delta Osx1}$ mice at 1-and 3-months of age. Representative image of femur metaphysis region at 1-month shows less trabecular bone in *Wwox*^{Osx1} mice. Quantitation of all µCT is shown in Fig S1A. **C**. Alkaline Phosphatase activity detects mature osteoblasts (left panel) and Alizarin Red staining (right panel) on *Wwox*$^{\Delta Osx1}$ and CTRL calvarial osteoblasts after 21 days in osteogenic media. **D**. Depletion of *Wwox* in bone, and no effect in liver levels in *Wwox*$^{\Delta Oc}$ mice. **E**. Significant decrease in trabecular number and connectivity density and a decrease in trabecular spacing at 3-months of *Wwox*$^{\Delta Oc}$ mice. Complete analysis is presented in Fig S1. **F**. Inhibition of osteoblast differentiation in the *Wwox*$^{\Delta Oc}$ mouse model.

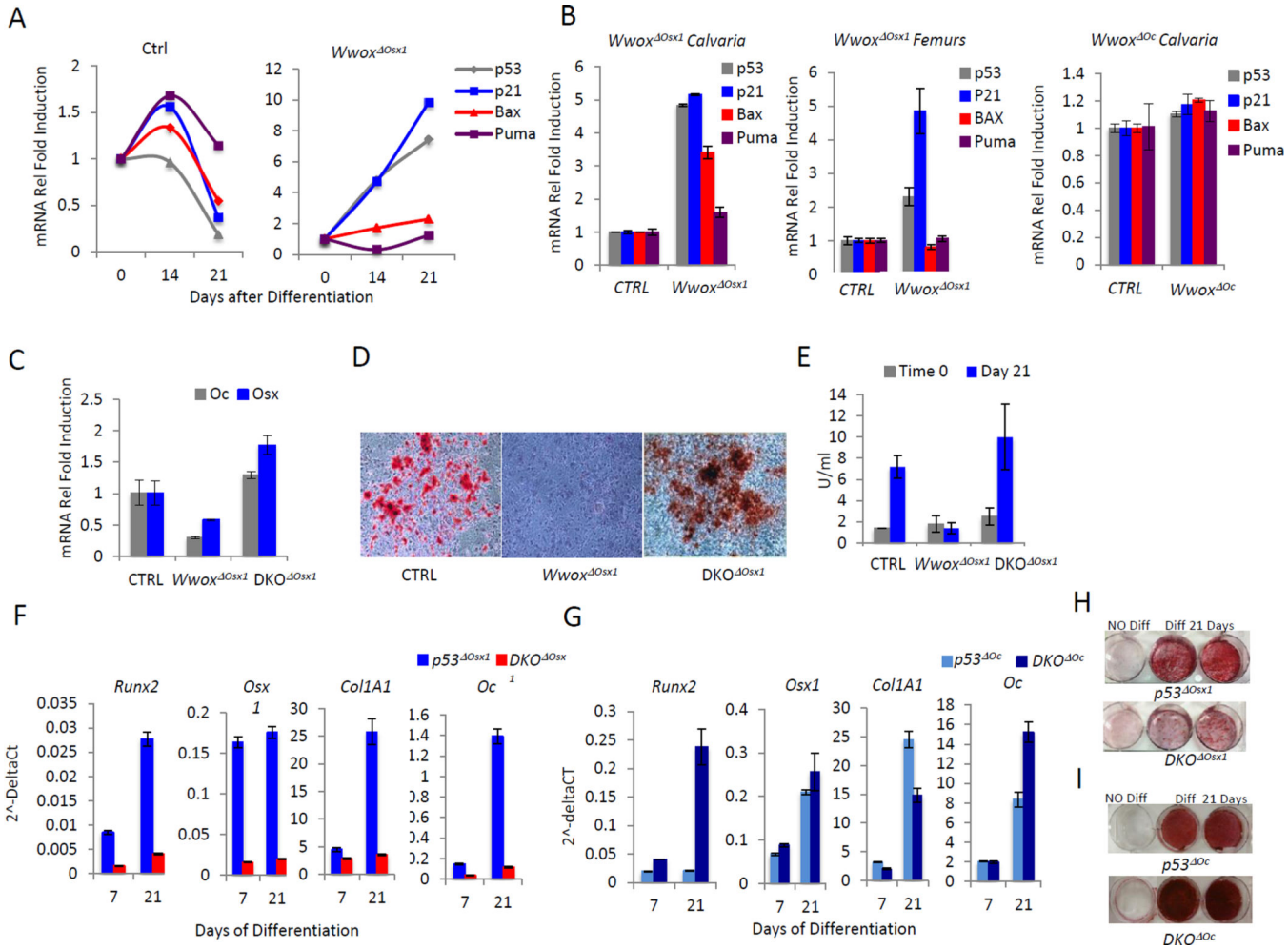

Figure 2. Defects in differentiation of *Wwox* deficient calvarial osteoblasts are partially rescued by p53 deletion

A. qPCR analysis on osteoblasts from *Wwox*$^{\Delta Osx1}$ calvaria showing an upregulation of cell proliferation and apoptosis regulators *Trp53, Cdkn1a (p21) Bax* and *Puma* mRNA levels during differentiation (days 0, 14, 21). **B**. Relative quantification of p53 and its target genes in control and *Wwox*$^{\Delta OB}$ calvarial osteoblasts at 21 days post-differentiation (left and right panel) and in 1 month-old *Wwox*$^{\Delta Osx1}$ femur bones (middle panel). **C**. qPCR analysis of *Osx1* and *Oc* levels in control, *Wwox*$^{\Delta Osx1}$ and *Wwox/p53*$^{\Delta Osx1}$ (*DKO*$^{\Delta Osx1}$) calvariae at 21 days of differentiation. **D,E** *Wwox*$^{\Delta Osx1}$ phenotype rescue by p53 deletion - Alizarin Red Staining of cells in C at day 21 and ALP activity in DKO cells are comparable to CTRL osteoblasts. **F,G**. Bone marrow derived p53$^{\Delta Osx1}$ mesenchymal stem cells (BMSCs) sustains, while DKO depletion inhibits osteogenesis. BMSCs were isolated from bone marrow of *p53*$^{\Delta Osx1}$ and DKO$^{\Delta Osx1}$ (F) and *p53*$^{\Delta Oc}$ and DKO$^{\Delta Oc}$ (G) mice and induced to differentiate in osteogenic media. qPCR analysis of RNA extracted after 7 and 21 days of differentiation for osteoblast markers. **H**. BMSCs from DKO$^{\Delta Osx1}$ mice show a reduced ability to form mineralized matrix than *p53*$^{\Delta Osx1}$ cells as assessed by Alizarin Red staining at 21 days from differentiation. **I**. DKO$^{\Delta Oc}$ BMSCs induced to differentiate show stronger osteogenic abilities than *p53*$^{\Delta Oc}$ cells.

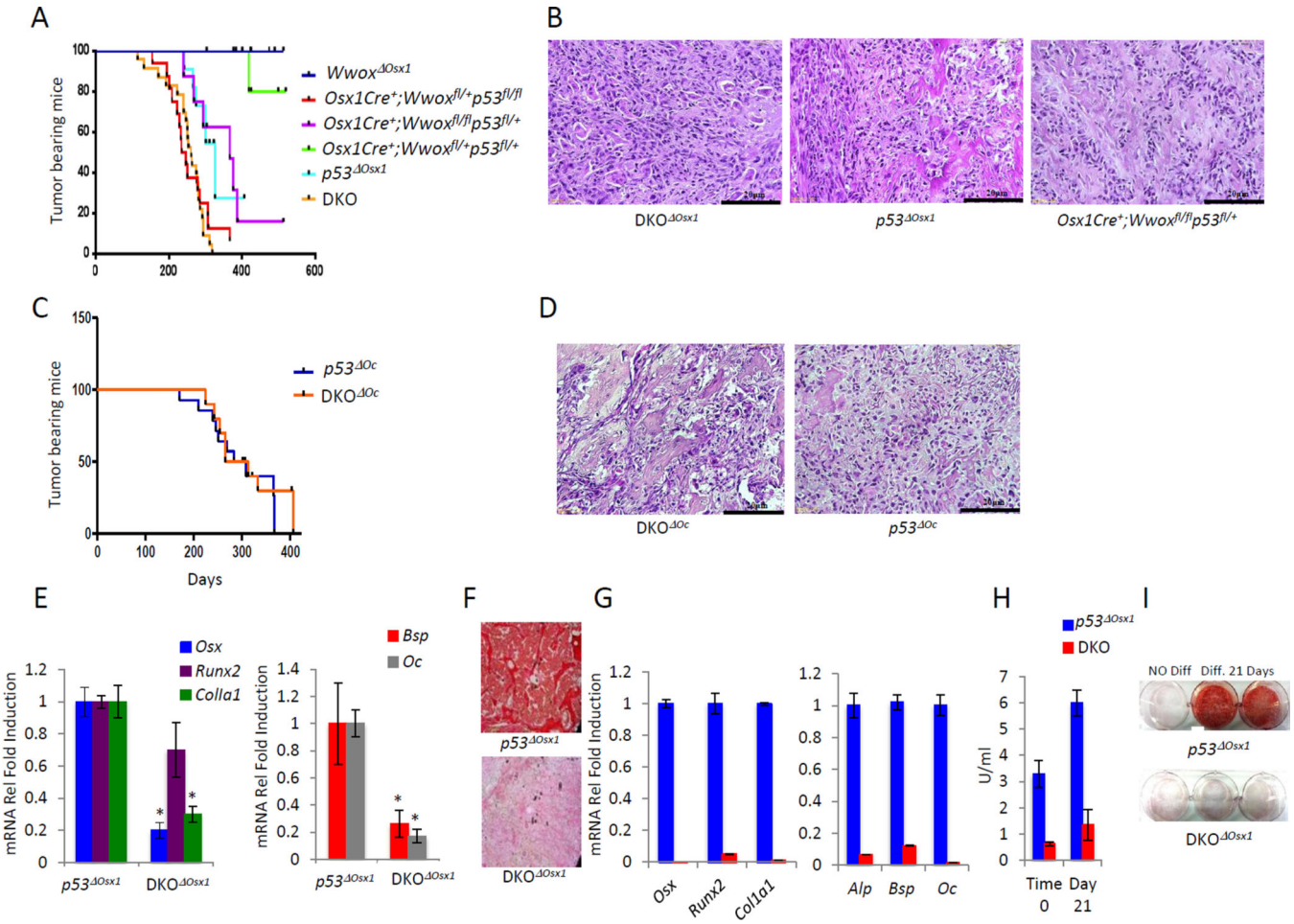

Figure 3. *Osx1-Cre* dependent deletion of *Wwox* results in the acceleration of osteosarcoma formation

A. Kaplan-Meier survival plots for the indicated genotypes. **B**. Histological sections of the tumors derived from $DKO^{\Delta Osx1}$ mice. Areas of pale staining represent bone tissues. **C**. Kaplan-Meier survival plots for $DKO^{\Delta Oc}$ and $p53^{\Delta Oc}$ mice. **D**. H&E staining of $DKO^{\Delta Oc}$ and $p53^{\Delta Oc}$ tumors. **E**. qPCR on $DKO^{\Delta Osx1}$ (n=7) and $p53^{\Delta Osx1}$ (n= 5) tumors. Osteogenesis makers were downregulated in $DKO^{\Delta Osx1}$ tumors when compared to $p53^{\Delta Osx1}$ tumors. **F**. Sirius-Red staining shows low collagen content in $DKO^{\Delta Osx1}$ tumors relative to $p53^{\Delta Osx1}$ tumors. **G–I**. Primary cell lines from $DKO^{\Delta Osx1}$ tumors show an inability to undergo osteogenic differentiation as assessed by qPCR (G) for markers of mature osteoblasts: ALP activity (H) and Alizarin Red staining (I) at day 0 and after 21 days of differentiation.

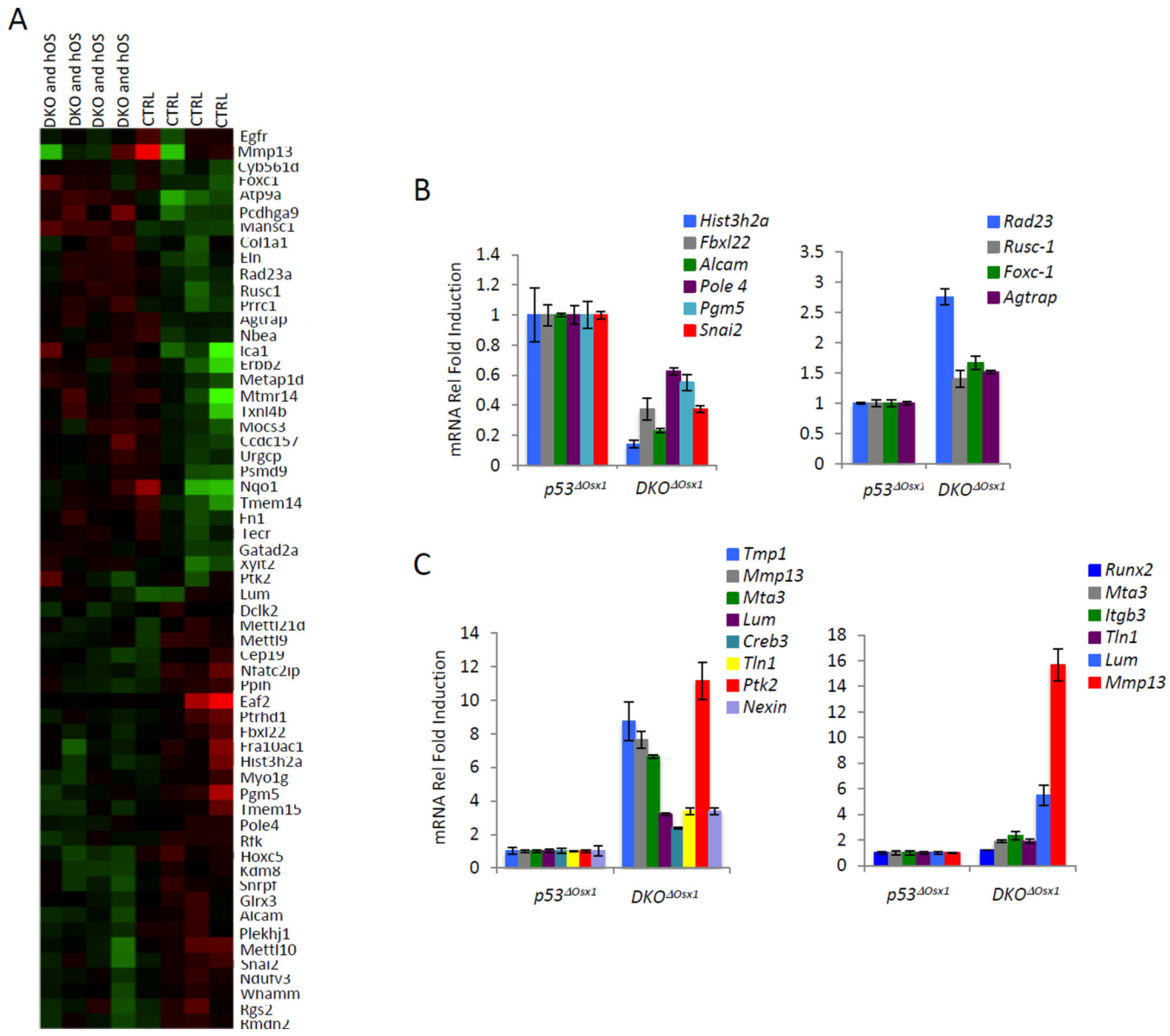

Figure 4. Transcriptomic analysis of *p53*$^{\Delta Osx1}$ and DKO$^{\Delta Osx1}$ tumors

A. Heat map generated from RNA-sequencing analysis shows the genes that are commonly altered in both *DKO*$^{\Delta Osx1}$ tumors and human OS samples compared to control bones. **B**. Validation by qPCR of several downregulated (left panel) and upregulated genes (right panel) in DKO tumors and hOS. **C**. Upregulation of RUNX2 target genes in DKO$^{\Delta Osx1}$ vs *p53*$^{\Delta Osx1}$ tumors (left) and tumor cell lines (right) as assessed by qPCR.

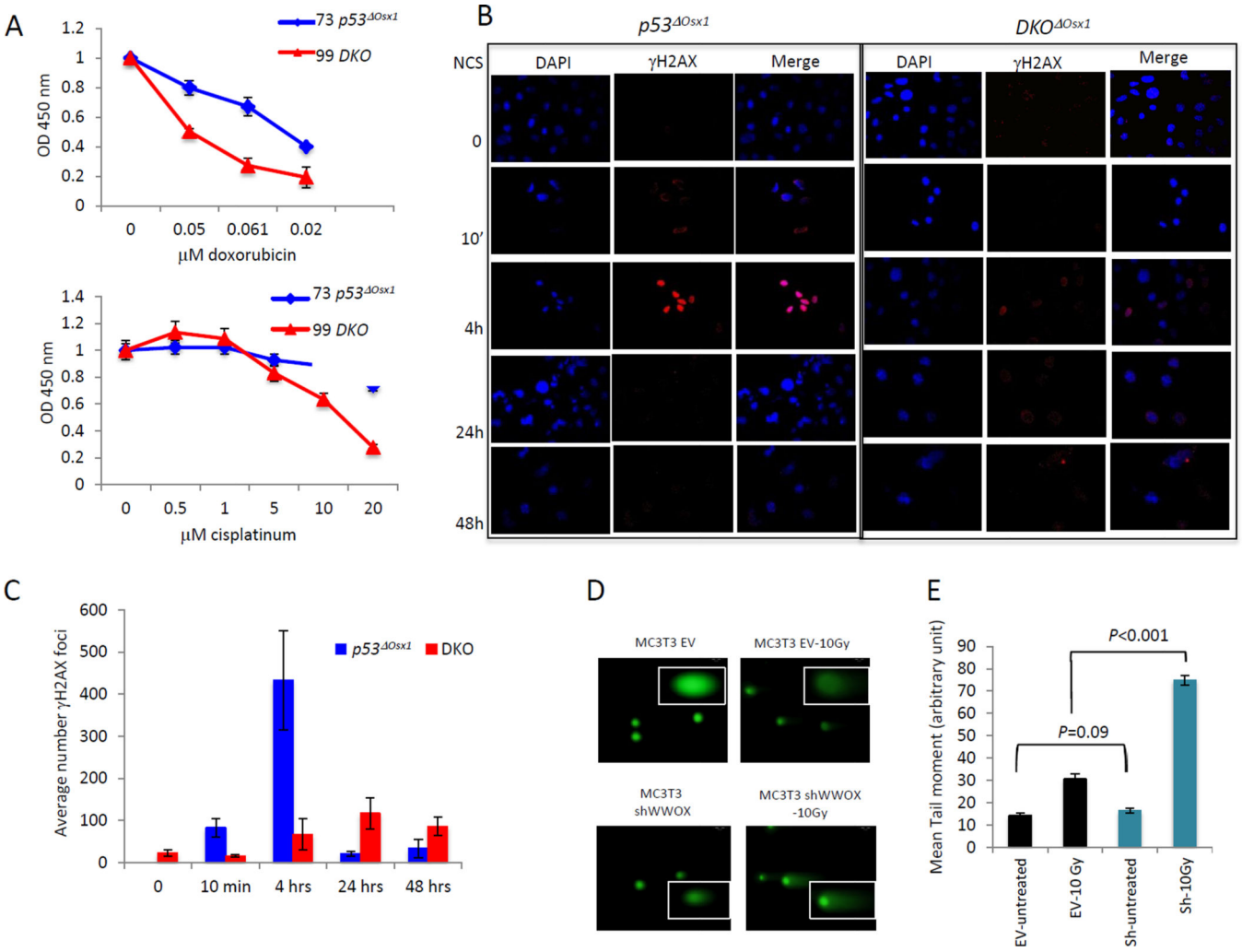

Figure 5. *DKO*$^{\Delta Osx1}$ tumors cells are more resistant to chemotherapy and display an impaired DDR

A. After 48h of treatment with increased concentration of doxorubicin and cisplatinum, DKO tumor cells present higher resistance than *p53*$^{\Delta Osx1}$ cells to the drugs as assessed by XTT assay. **B**. Immunofluorescence on DKO and *p53*$^{\Delta Osx1}$ tumor cell lines using anti γ-H2AX antibody and DAPI at different times after NCS treatment. **C**. Quantification of γ-H2AX staining from B. **D**. Comet assay. Control- (MC3T3 EV) and WWOX-depleted MC3T3 (MC3T3-shWWOX) cells were irradiated or not at 10Gy. Labeled DNA was visualized under a fluorescence microscope using 60× magnification. Representative images are shown. **E**. Quantification of the comet assay in D. Bars show the comet tail as measured using ImageJ 1.47g software.

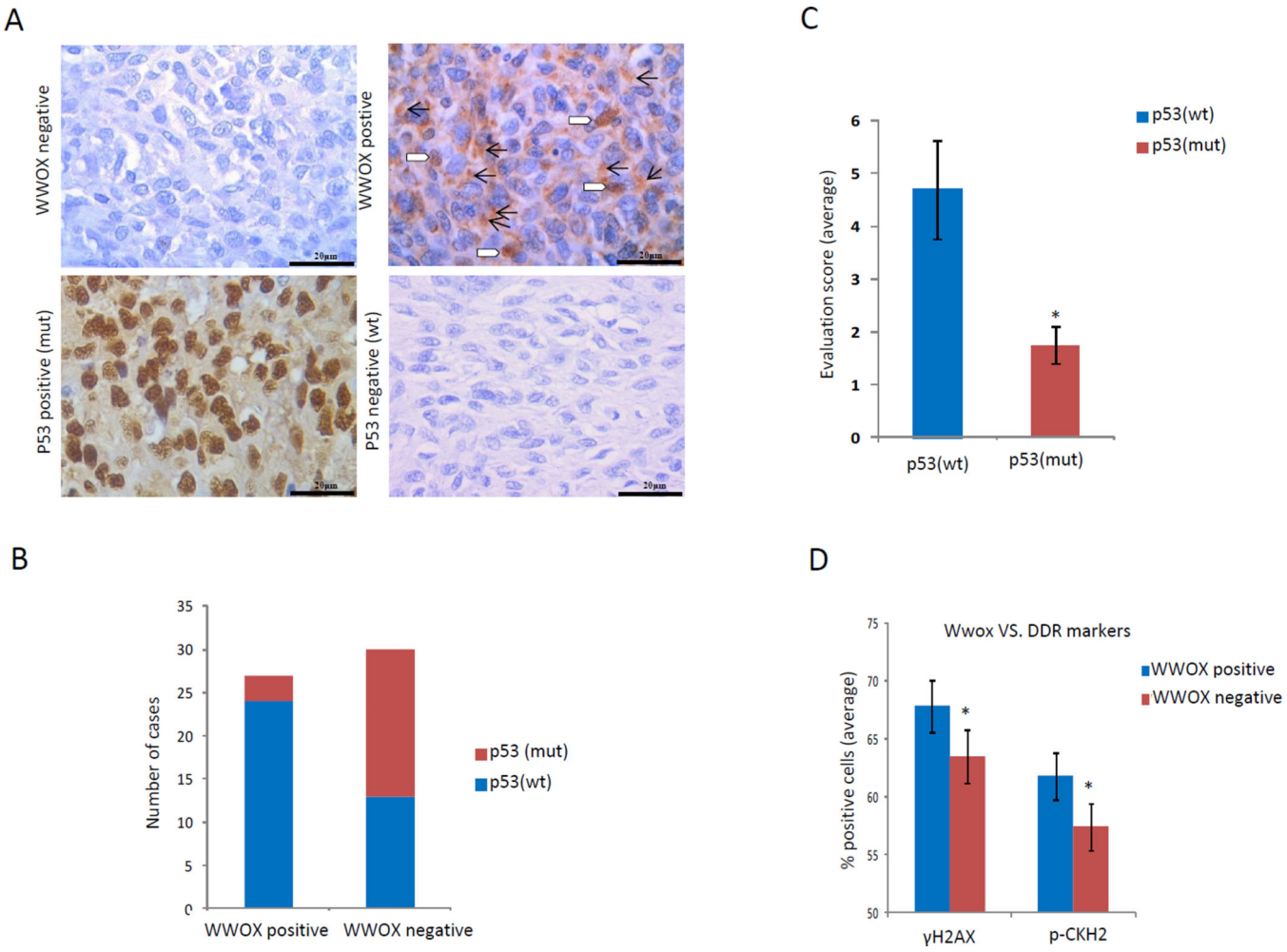

Figure 6. Loss of WWOX associates with inactivation of p53 and impaired DDR in human OS

A. Representative pictures of WWOX and p53 immunostaining in p53 wt or mutated p53 hOS. Scale bars: 20μm. Arrows and arrowheads depict cytoplasmic and nuclear WWOX immunopositivity, respectively. **B**. Quantitative representation of WWOX expression related to p53 status in hOS cases. **C**. Statistically significant comparison of WWOX immunohistochemical scoring values between p53 wt (average score=4,7) and p53 mut samples (average score=1,75). *$p<0.05$ **D**. Analysis of DDR markers, γ-H2AX and p-Chk2, in relation to WWOX expression in human OSs showing a clear trend of impaired DDR in WWOX negative cases and *vice versa*.